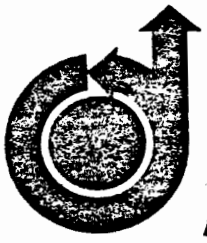

# AIAA-80-0088

# Electrical Interface Resistance and Potential Field Mapping of Explosive Bonded Interfaces

M. M. Yovanovich,
G. E. Schneider and V. S. Cecco,
University of Waterloo, Ontario,
Canada

**AIAA 18th**
**AEROSPACE SCIENCES MEETING**
January 14-16, 1980/Pasadena, California

# ELECTRICAL INTERFACE RESISTANCE AND POTENTIAL FIELD MAPPING OF EXPLOSIVE BONDED INTERFACES

M.M. Yovanovich*
G.E. Schneider#
V.S. Cecco+

Thermal Engineering Group
Department of Mechanical Engineering
University of Waterloo
Waterloo, Ontario

## Abstract

Increasing use of explosive bonding to join different metals has produced a need to examine the electrical characteristics of the resulting interface and the associated electrical resistance. This paper describes the potential probing technique used to obtain a complete map of the potential field and the interface resistance. The aluminum-iron interface examined has an rms surface roughness of 0.036 cm and an rms slope of 35 degrees. Several traverses were made at various locations along the outer surface of the two metals. The a.c. current had a frequency of 25 Hz and the current density ranged from 2 to 6 A/cm$^2$. It was observed that the interface resistance was $1.33 \times 10^{-6}$ ohm cm$^2$ $\pm$ 5 percent, independent of location of the traverse and of the current density. This result differs from that of Mengali and Seiler[1] who observed that the interface resistance depends upon the lateral position of the traverse. They observed differences of several hundred percent for lateral translations of 0.025 cm.

## Nomenclature

| | |
|---|---|
| $A$ | flow area |
| $I$ | electrical current |
| $J$ | current density |
| $\ell$ | effective specimen length |
| $N_i$ | number of interfaces |
| $R_c$ | constriction resistance |
| $t^*$ | equivalent metal thickness |
| $x$ | distance |
| $x_o$ | interface location |
| $\Delta x$ | incremental length |
| $V$ | voltage |
| $\Delta V_m$ | constriction voltage drop |

### Greek Letters

| | |
|---|---|
| $\alpha$ | angle between normal and surface current vector |
| $\delta$ | specific constriction resistance |
| $\rho$ | electrical resistivity |

### Subscripts

| | |
|---|---|
| 1,2 | metals 1 and 2 |
| Al | Aluminum |
| Fe | iron |
| TOT | total |

## Background

In today's production oriented society the search for fast, efficient bonding techniques is common to many facets of industry. In particular, the explosive bonding process is a direct consequence of a search for new and better methods of joining together dissimilar metals which cannot be joined by conventional methods. The art of explosive bonding has been developed to such an extent that many electrical and thermal systems currently find explosive bonded components in them.

The process involves the blasting of one material onto another with such force that the heat evolved at impact is sufficient to fuse the two materials at their common interface. Due to the large forces involved, however, plastic deformation occurs and a wavy interface results, the extent of which depends upon the materials being joined, the force at impact, and the component materials' relative orientation. The geometry of the interface produced is two-dimensional as a result of the method of fabrication and lends itself well to examination. Due to the increasing use of explosive bonded components it was felt that both the thermal and electrical behavior of such interfaces should be investigated. This research involves examination of one such sample; aluminum explosive bonded to

*Professor, Associate Fellow AIAA
#Assistant Professor, Member AIAA
+Engineer, Atomic Energy of Canada, Ltd.

iron*, Figure 8.

Results obtained from the testing of a second specimen, Aluminum on Copper, supports those obtained for the Aluminum-Iron combination. This indicates that the conclusions drawn in this paper may be extended to other similar interfaces. It remains the primary purpose of this paper, however, to alert other researchers and practising professionals in the field, of the capabilities of this particular research apparatus in determining both the resistance of, and the potential field surrounding, an explosive bonded interface; in particular this paper examines an aluminum-iron, explosion bonded interface.

## Background Theory

If the two contacting solids make continuous contact, as in explosive bonded interfaces, the flow lines refract at the interface due to the different component resistivities. This bending of the flow lines results in a constriction resistance. The incident and refracted angles must satisfy the following relationship:[2]

$$\rho_1 \tan \alpha_1 = \rho_2 \tan \alpha_2 \qquad (1)$$

where $\alpha_1$ and $\alpha_2$ are the local angles relative to the local normal to the interface and the respective electrical resistivities are $\rho_1$ and $\rho_2$, Figure 1.

As can be seen from Figure 2, the current flow lines converge and diverge as they cross a two-dimensional saw-tooth interface.[3] This plot of flow lines and equipotential lines was obtained with Teledeltos paper of resistivity ratio of 6.5:1. Figure 3 is a sketch of the anticipated flow lines and equipotential lines at a two-dimensional sinusoidal interface separating two metals whose electrical resistivities are $\rho_1$ and $\rho_2$ with $\rho_2 > \rho_1$.

Since the current is forced to follow a non-parallel flow path, an additional resistance exists and it is called the constriction resistance. The constriction resistance of a continuous contact interface is much smaller than that of a mechanical contact, Figure 4. When the interface is perfectly smooth and flat, the flow lines are parallel to each other and, always normal to the interface, and the constriction resistance is zero by definition.

## Description of Equipment

In this investigation a continuous a.c. potential-probing method was used in which an a.c. current of 25 Hz was passed through the sample of interest as shown schematically in Figure 5. Because of the extreme sensitivity required for most testing, DC current could not be used since it introduced inherent errors owing to the Seebeck thermoelectric potential generated at the probe-specimen contact and at the interface under examination.

The operating basis is that when a known current is passed through the specimen, the electrical resistivity of the material will create a potential difference between the two probes, Figure 6. One probe remains stationary at a reference potential while the other moves at a predetermined and constant speed, typically at 0.025 cm per minute. The signal is amplified with a differential amplifier, monitored with a wave analyser acting as both narrow-band-pass filter and rms meter, and registered continuously on a strip chart recorder.

The moving probe has a radius of about 0.0025 mm and is used to measure local potential distributions as it traverses the specimen surface. The probe begins its traverse in a region of uniform potential and constant potential gradient, moving across the disturbed zones (shown in Figure 3) surrounding the interface to another undisturbed region of constant potential gradient. The size of the disturbed region will depend on the interface roughness magnitude and therefore the scan length must be adjusted accordingly. The joint resistance is then measured by direct extrapolation from the undisturbed regions to the interface roughness center-line as seen in Figure 7.

The circuit consists of two major parts: the primary loop and secondary, potential measurement loop. The primary loop consists of a signal generator, power amplifier, load and calibration resistors, and the specimen. Current in this loop is usually less than three amperes but will vary with the sample size. The secondary loop contains the reference and potential measurement probe, a low voltage signal amplifier, and all the monitoring equipment.

Current determination is done by sampling the potential drop across a 0.1 ohm precision resistor and is usually checked both before and after each scan. The resistivity of OFHC copper was measured with this equipment at 24°C using a 0.245 x 0.387 x 1.90 cm sample. The resulting resistivity indicated $1.71 \times 10^{-6}$ ohm.cm compared to $1.69 \times 10^{-6}$ ohm.cm found in standard resistivity tables with correction for temperature.

## Measurement of Constriction Resistance

In the conventional method, voltage readings are taken at discrete locations and extrapolated to the interface. A pseudo-voltage drop ($\Delta V_m$) will be observed due to the resistance to current flow in the region of the interface, Figure 7. Since the measured $\Delta V_m$ will vary depending on the position at which measurement is made, the interface roughness centerline is arbitrarily selected as the reference datum. The pseudo-voltage drop and thereby the constriction resistance is then measured by extrapolating to the interface roughness centerline from the undisturbed regions of uniform potential gradient on each side of the interface. From the measured voltage drop a

*obtained from Dupont

specific constriction resistance can be calculated from the relation:

$$\delta = R_c A = \frac{\Delta V_m}{J} \qquad (2)$$

where J is the average current flux across the specimen cross-section. J = I/A, where I is the total current passing through the sample.

When examining explosive bonded interfaces, however, care must be exercised due to the unusually large interfacial roughness which may occur. In the sample under consideration, for example, the peak-to-peak roughness measured 0.127 cm, Figure 8. This is very large compared to the more common commercial surface roughnesses of typically 0.0023 cm peak-to-peak. For interfaces of this nature the material resistivities and resulting constriction resistances may appear to vary drastically with lateral displacement of the potential probe. However, if the range of testing is extended sufficiently far beyond the interface on either side, the potential gradient will approach a unique limit corresponding to that material's natural, undisturbed resistivity. This behavior is illustrated in Figure 9. Measuring the resistance from one undisturbed region, across the interface, to the other undisturbed region one should observe a unique resistance associated with any given interface.

This was substantiated by performing several scans under identical test conditions with the potential probes located at a different lateral position for each scan. The superposition of the five potential plots that resulted shows clearly that the constriction resistance is unique to the sample tested and has the same value regardless of lateral position. Figure 9 shows this superposition and also indicates to which lateral position each independent curve corresponds.

Pertinent data from this testing is listed in Table 1.

Table 1 Test parameters for the Aluminum-Iron Specimens

(i) Area = 0.460 $cm^2$

(ii) Current flux = 2.44 $A/cm^2$

(iii) Frequency = 25 Hz

(iv) Roughness data: rms height deviation = 0.036 cm
rms slope deviation = 35 degrees

(v) $\Delta V_m = 2.85 \times 10^{-6}$ volts

From this data the specific constriction resistance was calculated to be $1.31 \times 10^{-6}$ ohm. $cm^2$, measured at the roughness centerline.

Also worth noting here is the fact that all of the potential plots are enveloped by the undistributed resistivity extrapolation lines. This implies that the apparent resistivity seen locally near the interface is higher for both materials than the respective undisturbed material resistivity.

## Potential Mapping

Using this research apparatus, a complete mapping of the surface potential distribution is made possible by a method analogous to field plotting using Teledeltos paper. The basic method is described in the following paragraphs.

First a potential signal is found at any arbitrary longitudinal position but laterally on either edge. This potential is noted and its position plotted on square grid graph paper. The movable potential probe is then incremented laterally across the specimen width. At each increment the longitudinal probe position is adjusted to return the potential to its original value and the corresponding probe coordinates are plotted. A complete lateral traversal constitutes the generation of one equipotential line on the specimen surface.

This procedure is repeated for many different potentials until a complete surface potential map has been obtained. This mapping should extend sufficiently far beyond the disturbed zones, which are readily identifiable as shown by Figure 8, to establish reliable material resistivities.

A typical mapping for a current density of 6.0 $A/cm^2$ is presented in Figure 8 and clearly shows the potential distribution across a wavy explosive bonded interface and illustrates the effect of wavy surfaces on the electrical potential.

Mappings similar to that of Figure 8 were also obtained at current densities of 2.0 and 4.0 $A/cm^2$ with extremely similar results, thus confirming that the potential distribution and material resistivities are independent of the applied current density.

It is interesting to note that in the crest regions of the iron material the potentials are very close together and diverging on either side of these singular points. This indicates a local concentration of a very high resistivity material. This is better illustrated by superimposing the flow lines on the mapping as is done in Figure 3. It is readily apparent now that the current tends to remain longer in the lower resistivity aluminum than in the higher resistivity iron, and that it especially avoids the aforementioned regions of extremely high resistivity. It is postulated that these high resistivity regions may be the result of severe lattice distortion resulting from the bonding process, or from possible

material alloying.[6] The potential mapping of Figure 8 can also be used to determine the additional resistance due to flow line constriction near the interface.

By means of two potentials in the undisturbed region and the distance between them the material resistivities can be calculated with the known flow area. For prismatic members we have from ohm's law that:

$$\rho_{1,2} = \frac{1}{J} \frac{\Delta V_{1,2}}{\Delta x} \qquad (3)$$

where $\rho_1 \rho_2$ is the resistivity of material 1 and 2, $\Delta V_{1,2}$ is the measured voltage drop in material 1 and 2 over length $\Delta x$. This is done for both materials and the potential gradient is then extrapolated to the interface roughness centerline as before. Subtracting the material contributions from the overall resistance observed yields the constriction resistance by our definition as illustrated in Figure 10.

A sample data set and calculations are presented in Table 2.

Table 2 Test parameters for the Aluminum-Iron Specimens

(i) Area = 0.157 $cm^2$

(ii) Current flux = 2.0 $A/cm^2$

(iii) Frequency = 25 Hz

(iv) Roughness Data: rms height deviation = 0.036 cm
rms angle deviation = 35 degrees

(v) $\Delta V_{Fe} = 10.8 \times 10^{-6}$ volts

$\Delta V_{Al} = 2.3 \times 10^{-6}$ volts

$\Delta V_{TOT} = 35.9 \times 10^{-6}$ volts

(vi) $\Delta x_{Fe} = 0.25$ cm

$\Delta x_{Al} = 0.25$ cm

$\Delta x_{TOT} = 1.27$ cm

Using this data we can calculate the material resistivities. These are

$$\rho_{Fe} = 21.4 \times 10^{-6} \text{ ohm.cm}$$

and

$$\rho_{Al} = 4.5 \times 10^{-6} \text{ ohm.cm}$$

Knowing the resistivities and the overall voltage drop we immediately calculate the specific constriction resistances, defined by:

$$\delta = \frac{\Delta V_{TOT}}{J} - (\rho_1 \ell_1 + \rho_2 \ell_2) \qquad (4)$$

where $\ell_1 \ell_2$ are the lengths of $\rho_{1,2}$ on their respective side of the interface roughness centerline. For this example $\ell_1 = \ell_2 = 0.635$ cm and the calculated specific resistance is $\delta = 1.36 \times 10^{-6}$ ohm.$cm^2$.

These calculations were repeated for each of four additional current densities and the mean constriction resistance was determined to be $\delta = 1.33 \times 10^{-6}$ ohm.$cm^2$ with a standard deviation of less than 5.0 percent. This mean value agrees with the previous value of $1.31 \times 10^{-6}$ ohm.$cm^2$ obtained using the potential-distance plot within 1.6 per cent and we again confirm that the constriction resistance is unique regardless of lateral position of measurement or the current density used during the testing.

A second sample, aluminum explosion bonded to copper, was tested identically to the iron-aluminum sample. The resistivity ratio of component materials was only 1.38 in this case and the rms roughness only 0.018 cm. As a result the flow line diffraction was not as severe and the resulting constriction resistance was smaller in magnitude. The specific interfacial resistance obtained was $\delta = 2.02 \times 10^{-7}$ ohm.$cm^2$ indicating this behavior.

To facilitate more diversified application of test results an Effective Constriction Resistance Length (ECRL) is introduced which presents the specific constriction resistance as an equivalent thickness,[4] t*, of material of a composite resistivity and is defined by:

$$t^* = \delta / \sum_{i=1}^{n} N_i \rho_i \qquad (5)$$

where $N_i$ is the number of interfaces with $\rho_i$ on either side. For the case under consideration there is only one interface and equation (5) reduces to:

$$t^* = \delta / (\rho_1 + \rho_2) \qquad (6)$$

Using this expression the equivalent thickness of the aluminum-explosion-bonded-to-iron system is 0.050 cm based on the potential plot and 0.051 cm based on the potential mapping. This means physically that the interface has the same effect as adding .050 cm of each material to the system, and is a convenient method of accounting for the interfacial resistance in design and analysis such that the computational labor in such cases is reduced. It also allows for application to both thermal and electrical systems provided the material conductivity ratios are nearly the same. For pure materials of course this is usually the case and frequently for alloys of low dilution.

## Discussion and Conclusions

It was the intent of this paper to illustrate the capabilities of the research apparatus herein described, and especially its application to mapping the potential field of an explosive bonded interface and the determination of its electrical constriction resistance.

It is possible now to avoid theorizing the behavior of an interface in an electrical circuit since it can be directly observed using the potential probing apparatus. However, sample size is limited to that which will provide sufficiently large voltage signals for detection, using available current sources, while still ensuring that the sample is typically representative of the interface in question.

Application of the apparatus to an aluminum-iron explosion bonded interface has shown that the flow lines do indeed refract at the interface and that the region of non-uniform flow appears to extend equally far on both sides of the interface centerline.

More important is the verification that the constriction resistance presented by this interface is independent of the lateral position of measurement or the current density used for testing. Differences in local interface position are compensated for by changes in the surrounding materials' apparent resistivities. This is a result of local current density variations and causes the resistance between the regions of undisturbed and uniform potential field to be constant.

## Acknowledgement

The authors acknowledge the financial support of the National Science and Engineering Research Council of Canada. One of the authors (Cecco) acknowledges the support of the Atomic Energy of Canada Limited.

## References

[1]Mengali, C.J. and Seiler, M.R., "Contact Resistance Studies on Thermoelectric Materials," Advanced Energy Conversion, Vol. 2, pp. 59-68, 1962.

[2]Smythe, W.R., "Static and Dynamic Electricity," McGraw-Hill Book Company, New York, 1968, p. 20.

[3]Thibeault, R., "Electrical Resistance Across a Two-Dimensional Saw Tooth Interface; Using Teledeltos Paper", ME-82 Project, University of Waterloo, 1971.

[4]Cecco, V.S., and Yovanovich, M.M., "Electrical Measurement of Joint Resistance at Perfect Contact Interfaces: Application to Thermal Joint Conductance," AIAA 10th Aerospace Sciences Meeting, January 1972, paper no. 72-19.

[5]Mueller, J.J. and Eggers, P.E., "Diagnostic Analysis Techniques for Use on Thermoelectric Elements," 1971 Intersociety Energy Conversion Engineering Conference Proceedings, pp. 956-962, Boston, Mass., August 3-5, 1971.

[6]Van Vlack, L.H., "Materials Science for Engineers," Addison-Wesley Publishing Company, 1970, pp. 285-6.

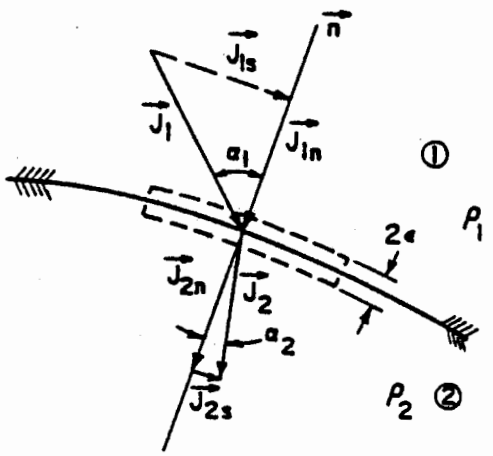


Fig. 1 Refraction of flow lines across a continuous contact interface $\rho_2 > \rho_1$.

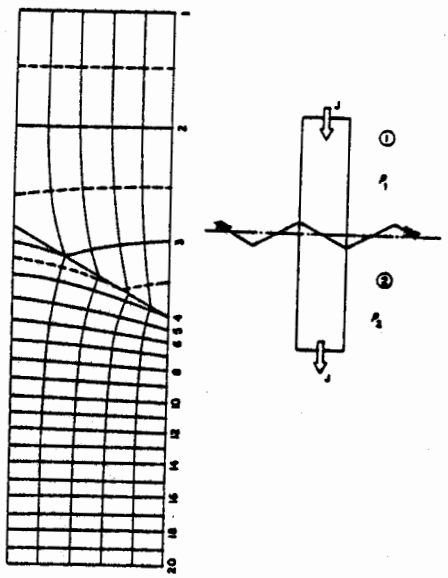

Fig. 2 Flow lines and equipotential lines for a two-dimensional saw-tooth interface $\rho_2/\rho_1 = 6.5$.

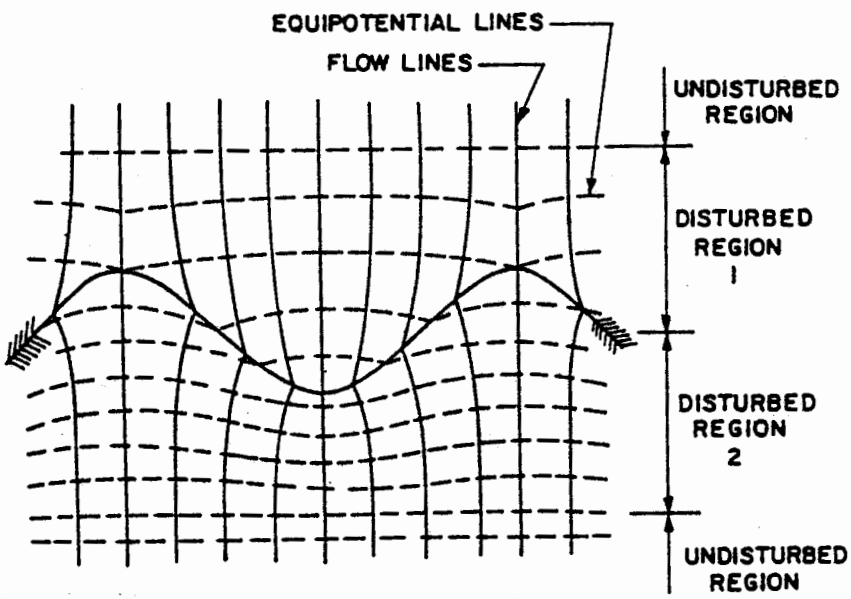


Fig. 3 Constriction of flow lines at a continuous contact interface $\rho_2 > \rho_1$.

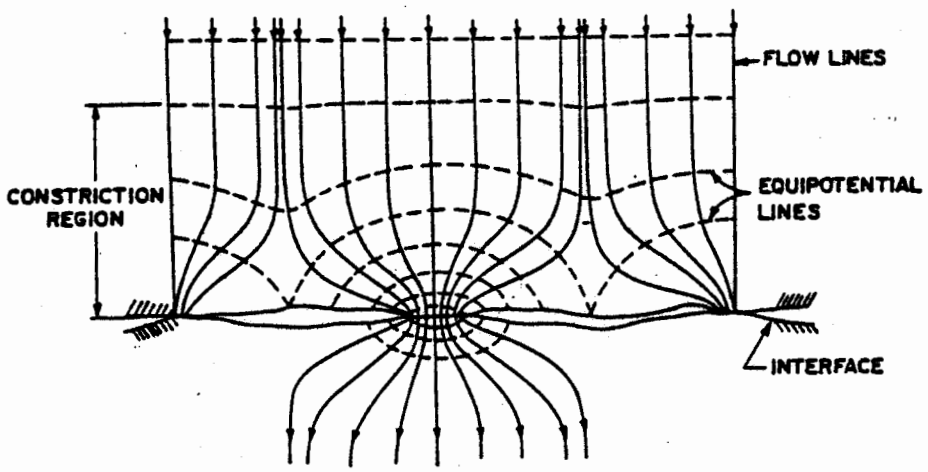


Fig. 4 Constriction of flow lines at a mechanical contact interface.

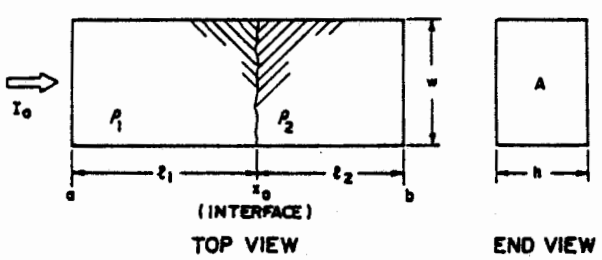


Fig. 5 Current flow through a typical specimen.

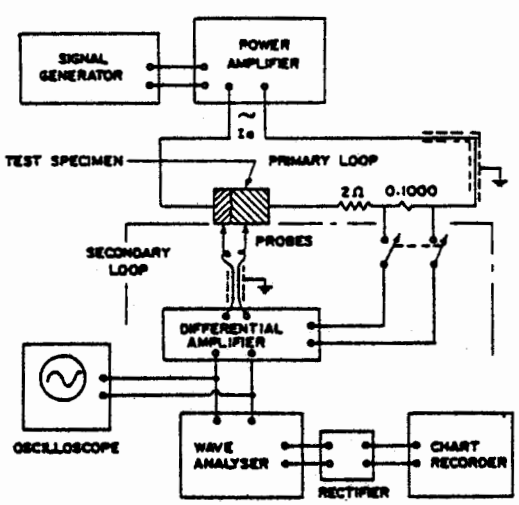


Fig. 6 Schematic of potential-probe apparatus using ac current.

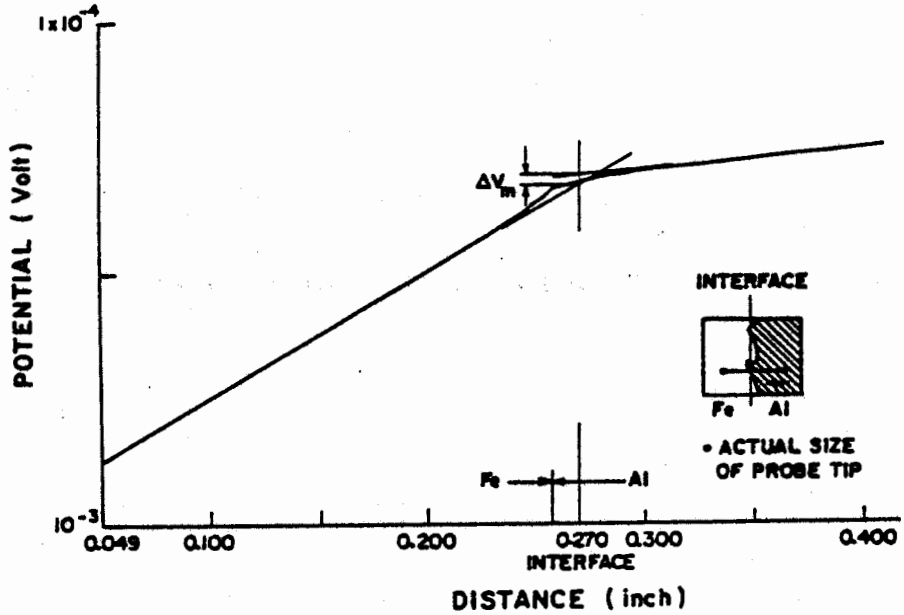


Fig. 7 Typical voltage versus distance distribution.

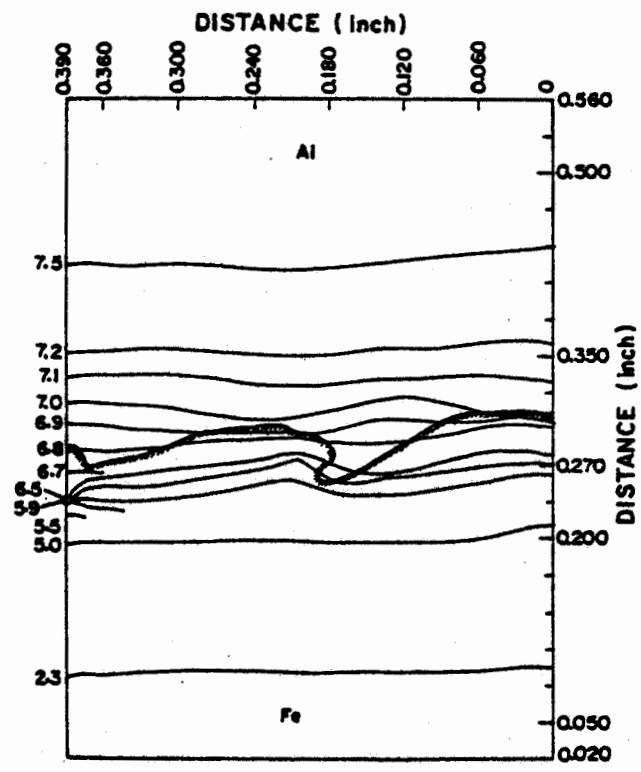


Fig. 8 Continuous potential mapping of the top surface of the Fe-Al explosive bonded specimen.

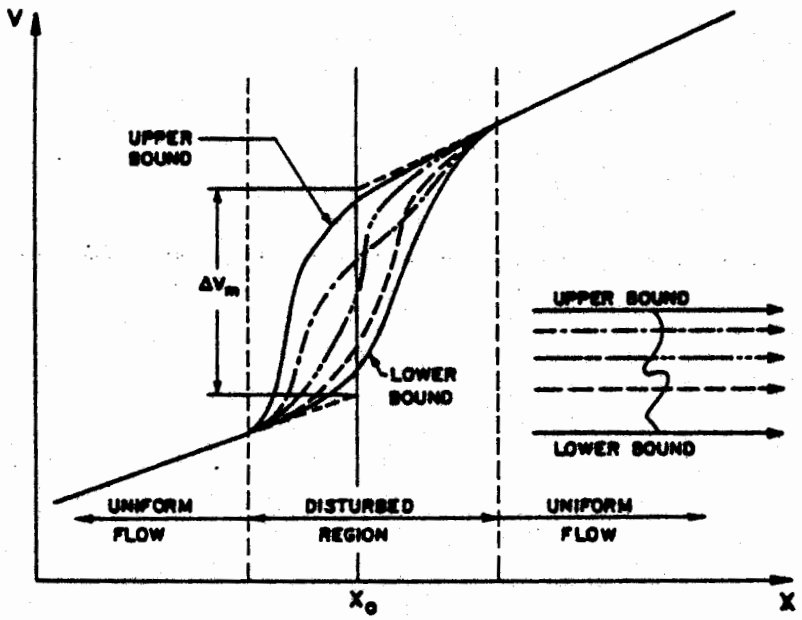


Fig. 9 Voltage distributions across a continuous contact explosive bonded specimen.

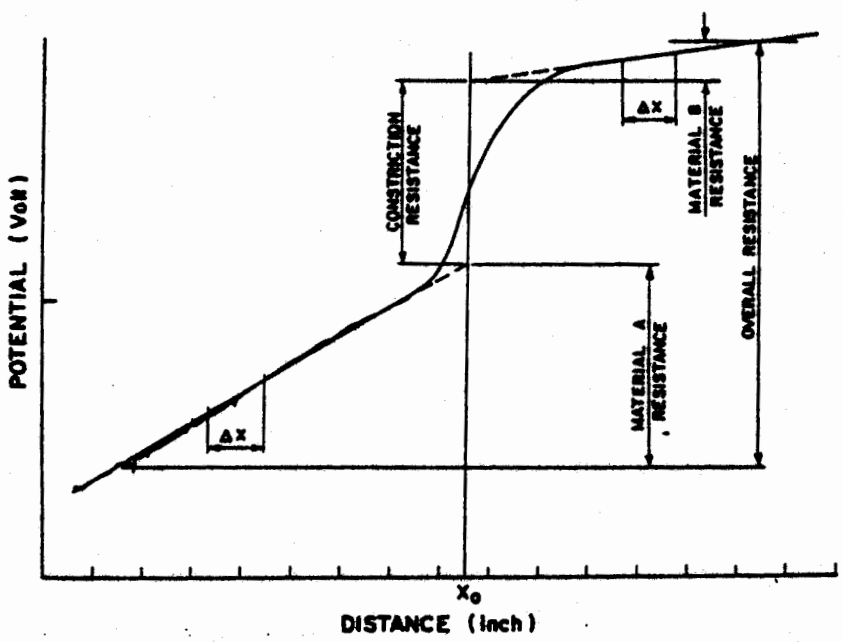


Fig. 10 Contributions to the overall observed voltage drop.